THE ASTROPHYSICAL JOURNAL, 493:180–194, 1998 January 20

STAR FORMATION IN R136: A CLUSTER OF O3 STARS REVEALED BY *HUBBLE SPACE TELESCOPE* SPECTROSCOPY[1]

PHILIP MASSEY
Kitt Peak National Observatory, National Optical Astronomy Observatories,[2] P.O. Box 26732, Tucson, AZ 85726-6732
AND
DEIDRE A. HUNTER
Lowell Observatory, 1400 West Mars Hill Road, Flagstaff, AZ 86001
Received 1997 June 10; accepted 1997 August 29

ABSTRACT

The R136 cluster in 30 Doradus is the prototype "super star cluster," and the only example sufficiently close that its massive star content can be studied directly. We have used the *Hubble Space Telescope* to obtain spectra of 65 of the bluest, most luminous stars in R136 and find that the majority of these stars are of type O3, the hottest, most luminous, and most massive stars known. The total number of O3 stars in this one cluster exceeds the total number known elsewhere in the Milky Way or Magellanic Clouds. The highest luminosity stars found are O3 If*, O4 If+, O3 If/WN6-A, and H-rich WN stars, with masses in excess of 120 $\mathcal{M}_\odot$, the highest masses for which appropriate evolutionary tracks are currently available. In accord with de Koter, Heap, & Hubeny, we conclude that these WN stars must be core H-burning stars whose spectra are WR-like because of high luminosity, and we find that their individual luminosities are a factor of 10 higher than is normal for WN stars of similar type but are like those found in the Galactic cluster NGC 3603, which they also resemble spectroscopically. Our spectroscopy does include stars as late as B0 V and samples most stars in the core of the R136 cluster with masses $>50\ M_\odot$. The spectroscopy has been combined with *HST* photometry to study the star formation history and initial mass function of the R136 cluster. The young age (<1–2 Myr) for the highest mass stars, combined with what was previously known for the intermediate-mass populations, suggests that the lower mass stars began forming 4–5 Myr ago and continued forming until the high mass stars formed, consistent with the paradigm in which the formation of massive stars shuts down further star formation in the molecular cloud. Despite the unique preponderance of the highest mass and luminosity stars ever seen, the initial mass function (IMF) is found to be completely normal, with a slope $\Gamma = -1.3$ to -1.4. The number of high-mass stars is in good accord with that predicted by the IMF of the intermediate-mass stars, suggesting that a Salpeter-like IMF holds over the mass range 2.8–120 $\mathcal{M}_\odot$ within the R136 cluster. The fact that the IMF slope in R136 is indistinguishable from those of Galactic and Magellanic Cloud OB associations suggests that star formation produces the same distribution of masses over a range of ~200 times in stellar density, from that of sparse OB associations to that typical of globular clusters. The large number of O3 stars in R136 is then simply a consequence of its youth (<1–2 Myr) and its richness, suggesting that the upper mass "cutoff" to the IMF seen in OB associations may simply be the result of their sparcity.

Subject headings: open clusters and associations: individual (R136) — stars: early-type — stars: luminosity function, mass function

1. INTRODUCTION

R136 is the central object at the heart of the 30 Doradus nebula in the Large Magellanic Cloud. Once thought to house a single supermassive star, R136 has proven to be even more interesting—the core of a "super star cluster." *Hubble Space Telescope* (*HST*) images reveal over 3500 stars (of which 120 are blue and are more luminous than $M_V \sim -4$) within the boundaries of the 35″ Planetary Camera (PC2) field of view, with the majority of the stars located within an 8″ (2 pc) radius of the semistellar R136 core (Hunter et al. 1995). Similarly extreme objects have now been recognized in more distant galaxies and may in fact be the young analogs of globular clusters (O'Connell, Gallagher, & Hunter 1994; O'Connell et al. 1995; Hunter, O'Connell, & Gallagher 1994). As the prototype of such objects, the R136 cluster is the only one sufficiently close by that its stellar population can be studied directly.

We are interested in the star formation history and the initial mass function (IMF) of such an extreme star-forming event. Studies of Galactic and Magellanic Cloud OB associations have shown that the slopes of the IMF are indistinguishable among the clusters studied (Massey et al. 1995a, 1995b), with an IMF slope nearly Salpeter ($\Gamma = -1.3$). Nevertheless, stars born as part of more modest events, the "field" O and B stars, have an IMF slope that is considerably steeper ($\Gamma \approx -4$). The R136 cluster has a stellar density ~200 times greater than that of a typical OB association. Will R136 prove to be top heavy in extremely massive

[1] Based on observations with the NASA/ESA *Hubble Space Telescope*, obtained at the Space Telescope Science Institute (STScI), which is operated by the Association of Universities for Research in Astronomy, Inc., under NASA contract NAS 5-26555.

[2] NOAO is operated by the Association of Universities for Research in Astronomy, Inc., under a cooperative agreement with the National Science Foundation.

stars, indicative of a flat IMF? Hunter et al. (1995, 1996) studied the IMF of the intermediate mass stars (2.8—15 $\mathcal{M}_\odot$) in R136 and found an IMF slope that was only slightly shallower ($\Gamma \sim -1$) than Salpeter even within the core of the cluster. However, despite the addition of ultraviolet photometry (Hunter et al. 1997), little can be said about the more massive and luminous stars in the R136 cluster on the basis of photometry alone, as the colors of stars hotter than $T_{\rm eff} \sim 30{,}000$ K are degenerate with temperature (Massey et al. 1996), and an accurate knowledge of the temperature is needed for determining the bolometric luminosity of a star and hence its mass.

For this reason, we undertook optical stellar spectroscopy of 65 of the brightest, bluest stars in the R136 cluster using the Faint Object Spectrograph (FOS) on *HST*. Spectroscopic studies have previously been made with the FOS and the Goddard High-Resolution Spectrograph (GHRS) for four stars in the R136 region: R136a1 and R136a2 (whose light contaminates each other even with *HST*), R136a3, and Mk 42 (Walborn et al. 1992; Heap et al. 1994; de Koter, Heap & Hubeny 1997), but otherwise spectral studies of individual stars have concentrated on regions away from the central cluster, where crowding is presumed to be manageable (Melnick 1985; Parker 1993; Walborn & Blades 1997, and references therein). Such studies have shown that the 30 Doradus region is extremely rich in massive young stars, but we were unprepared for the plethora of the absolute hottest and most luminous stars revealed by our *HST* spectroscopy.

2. OBSERVATIONS

Our stars were chosen on the basis of the Hunter et al. (1997) photometry, with the faintest stars corresponding roughly to what we expected for a 20 $\mathcal{M}_\odot$ zero-age main-sequence star (F170W $\approx$ 14.5; F555W $\approx$ 16.5). In such an extremely crowded region, there will always be some multiple objects that cannot be resolved even with the power of *HST*, but in order to obtain the cleanest sample we could, we eliminated any stars from consideration if they had a detected companion less than 1.5 mag fainter within 0.″16 (3.5 pixels), slightly larger than the 0.″13 radius of the spectrograph's entrance aperture. This list contains 130 stars, and it was our intention to observe a complete sample down to F555W $\approx$ 16 and a sampling of fainter stars. We were originally assigned 30 Continuous Viewing Zone orbits (CVZs) for this program, but, because of various scheduling difficulties, we were able to observe only 15 CVZs plus 8 regular orbits. Thus our spectroscopy is complete only to F555W = 14.8, 85% complete at F555W = 15.5, and no stars have yet been observed fainter than F555W = 15.8, although additional spectroscopy is currently planned.

We chose to determine effective temperatures for our stars by assigning classical spectral types using the optical region, rather than by attempting to observe in the UV. Although hot stars have considerably more flux in the UV, the moderately high reddening [$E(B-V) \approx 0.4$] combined with the relatively poor throughput of *HST* at shorter wavelengths rendered UV observations of so many stars out of the question. We used the G400 FOS/RD configuration with the 0.″26 diameter aperture to obtain wavelength coverage from 3250 Å to 4820 Å with 3 Å resolution. The data were obtained in the default "quarter-stepping" mode, in which the spectra are moved across five adjacent diodes in increments of one-quarter diode, in order to reduce the effects of dead diodes. We aimed for a minimum signal-to-noise ratio (S/N) of 60 per 3 Å resolution element at 4400 Å, near the principal classification lines for O-type stars.

In order not to degrade the S/N, we had to center our targets to 0.″04 within the 0.″26 diameter aperture; this placed stringent requirements both on our coordinates and our observing procedures. We measured our coordinates using the PC2 images from which the Hunter et al. (1997) photometry was derived, with comparisons made to exposures taken at three different epochs in order to check for any systematic problems. Although it takes significant overhead (46 minutes) to center a star at the 0.04″ level, *HST* is capable of very accurate blind offsetting. We therefore chose to observe our program stars by first centering upon an isolated nearby star and then observing several program stars by blind offsetting, recentering on the offset star every few orbits. This procedure appeared to work well: the observed fluxes match those expected on the basis of the stars' magnitudes, and the S/N achieved in practice was always close to what we expected, even for the very high S/N $\sim$ 90 observations.

The classification was occasionally complicated by the idiosyncrasies of the FOS, most notably bad diodes. A dead diode that has been turned off on the spacecraft has little effect on the observed spectra because of the standard way that the data are obtained via overstepping. (Each pixel in the final spectrum has been averaged over 5 adjacent diodes [20 pixels]; if one of these is turned off, then the S/N will be degraded but the spectra will be otherwise unaffected.) However, a dead diode that has not been deactivated results in a spurious absorption feature extending over 20 pixels. Similarly, a "noisy" diode will lead to a spurious emission feature extending over 20 pixels. Often these diode problems are intermittent. Such problems resulted in an occasional false emission peak at λ4046, which we were careful not to confuse with true N IV λ4058 emission, an occasional false emission peak at λ4325, giving Hγ an inverse P Cygni profile appearance, and an occasional broad, shallow absorption feature centered at λ4485, which could affect the longward side of the He I λ4471 line. Fortunately, the effects of bad diodes can be recognized as they are always 20 pixels in width, with relatively sharp edges; examination of the wavelength of suspected features was also illuminating. Although we utilized the standard pipeline reductions of the spectra, the flat field used for the reductions was also examined in order to better understand the level at which we could trust the data.

Altogether we obtained spectral types for 65 stars in the R136 cluster, including our offset star Mk 34. (The spectrum of this star was not overstepped but was obtained for "free" as part of the centering process.) Because of the need for accurate centering, we reobserved two stars observed by de Koter et al. (1997), Mk 42 (our star R136-002) and R136a5 (=R136-20). We did not attempt to reobserve R136a1 or R136a2, as they were too close to each other for additional observations to improve upon the work of Heap et al. (1994) and de Koter et al. (1997); we will discuss these two stars later in § 3.7. We show in Figures 1 and 2 the location of all of the 67 stars in the R136 cluster with *HST* spectroscopy. The identification numbers are the same as given in Hunter et al. (1997), except for two stars (H96-28 and H96-59) which were just out of the field of view during the

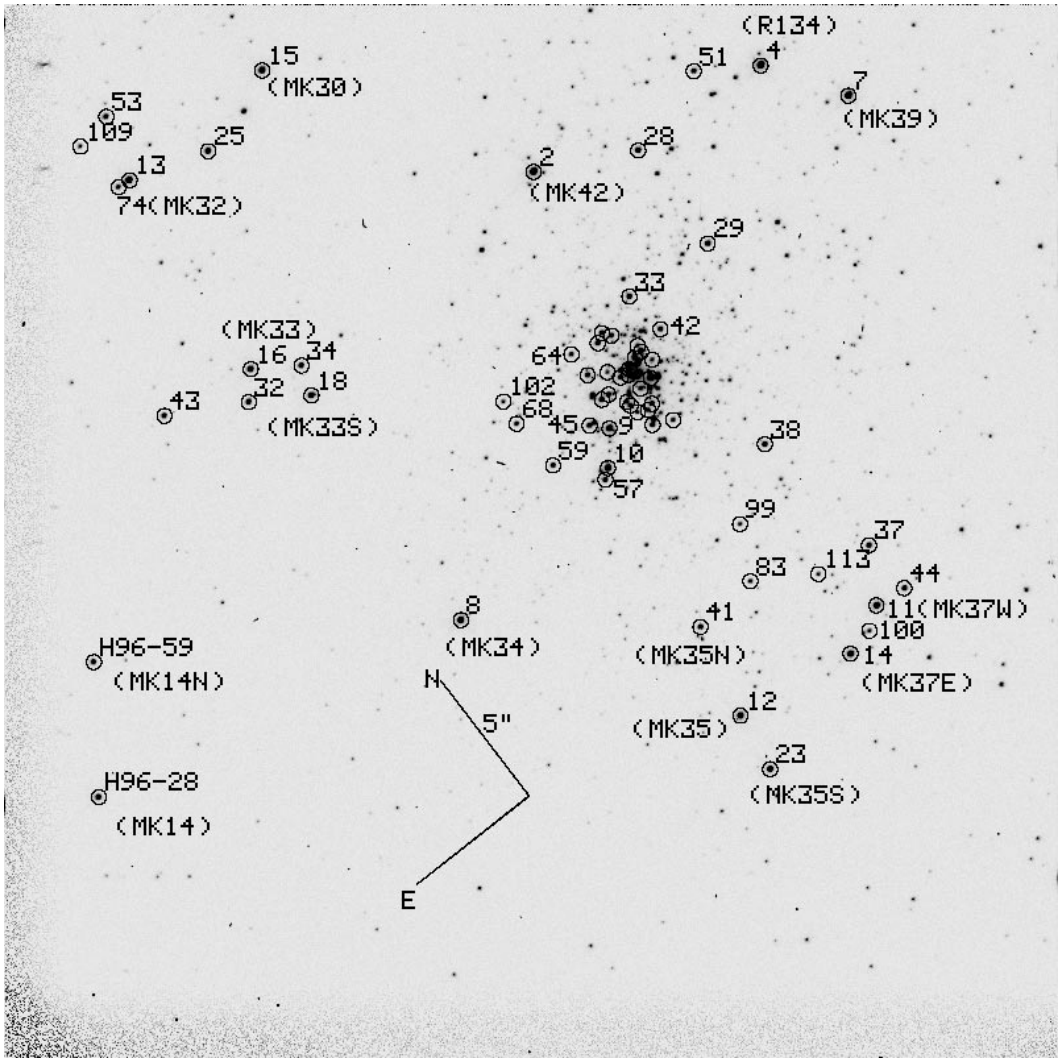

FIG. 1.—Full 35″ × 35″ PC2 field showing the R136 cluster. The image is "u2hk0302t," a 3 s exposure with the F555W filter obtained in 1994 September with the WFPC2 camera on *HST*. Stars observed spectroscopically are circled. The identification numbers are from Table 1, along with their Melnick (1985) numbers. (The identification of stars in the central portion are given in Fig. 2.) The size of the circles are roughly twice the diameter of the entrance aperture used for the spectroscopy.

F170W observations, but whose F336W–F555W colors determined from other observations (Hunter et al. 1996) suggested they were of early type.

3. THE SPECTRAL TYPES FOUND IN THE R136 CLUSTER

The spectra were classified using the precepts of the Walborn & Fitzpatrick (1990) spectral atlas, with additional reference to Walborn (1982) and Conti (1988) for the "transition type" O3 If*/WN6-A. We list our spectral types in Table 1, and the significant finding of our study is immediately apparent: *the vast majority of the stars we've observed are of type O3!* These are the hottest and include the most luminous and most massive stars known. We include in Table 1 the distance from the center of the cluster in parsecs and the absolute visual magnitude (M_V), which we will derive in § 5 after correcting for reddening. A distance modulus of 18.5 has been assumed throughout.

The optical classification of O-type stars is based primarily on the relative strengths of He I and He II, with He I λ 4471 and He II λ4542 equal at type O7.5, and negligible He II present by type B0. The extension of the classical MK spectral types to include "O3" was originally necessitated by four stars in the η Carina region (Walborn 1971). Their spectra showed no He I at modest resolution and widening on photographic spectrograms, suggesting that they were hotter than the earliest type stars (O4) known at that time. As of 1993, only 27 O3 stars had been confirmed in the LMC, SMC, or Milky Way (Walborn 1994). Higher S/N, better resolution observations have succeeded in detecting He I in some of these stars but not in others (Kudritzki 1980; Simon et al. 1983; Puls et al. 1996). Thus we know that the O3 classification (which is degenerate in the sense of being bounded only on the low-temperature side) spans a range in effective temperature and hence bolometric correction (Puls et al. 1996). We will return to this point in § 5. The luminosity classification of O-type stars is based primarily on the He II λ4686 line strengths at early types, with strong emission indicative of supergiants and strong absorption indicative of luminosity class "V."

3.1. *The O3 Supergiants*

Eight of our R136 stars are classified as O3-type supergiants (O3 If*). O3 supergiants are distinguishable from

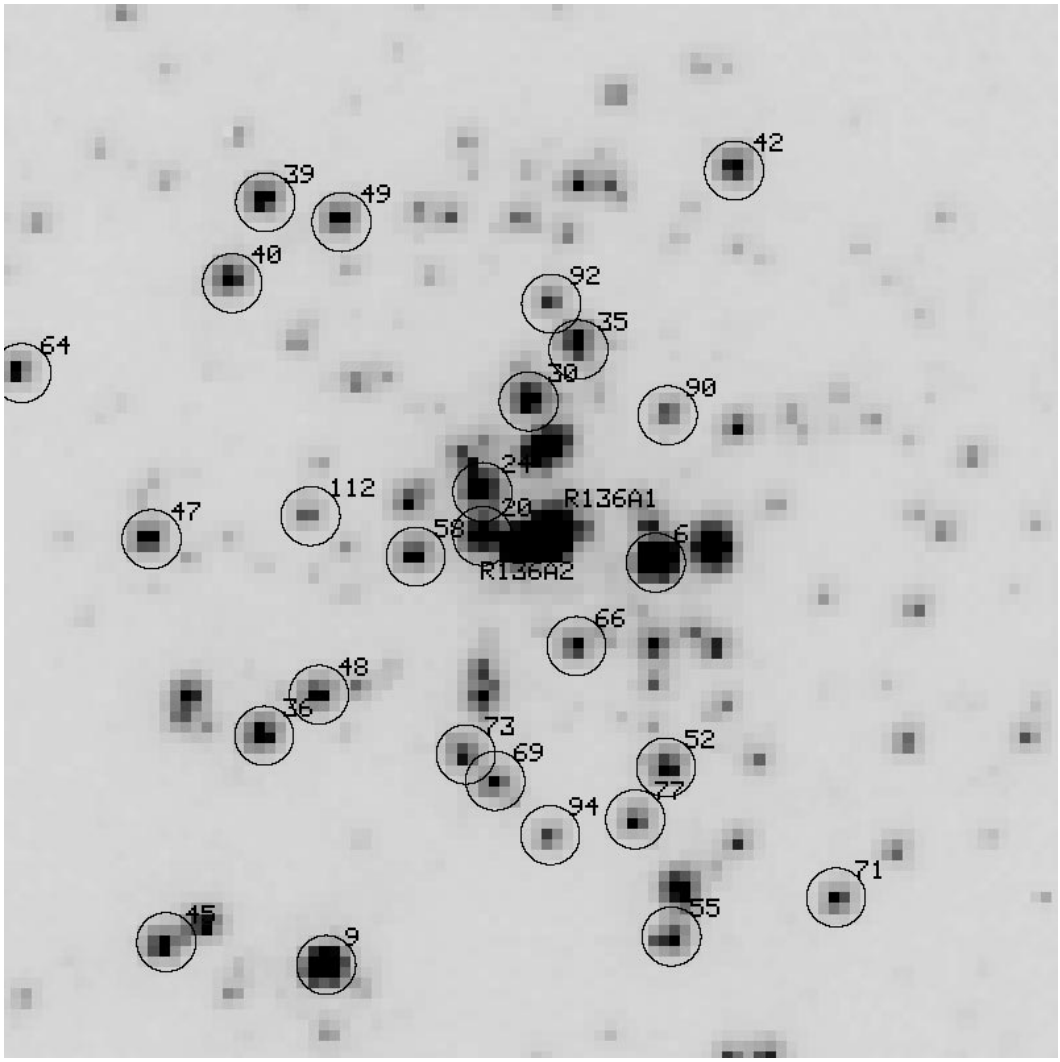

FIG. 2.—The central 4″.55 × 4″.55 portion of Fig. 1. The identification of the stars observed spectroscopically is given. The size of the circles correspond to the 0″.26 diameter entrance aperture of the FOS. The "R136a1" and "R136a2" components are indicated.

lower luminosity O3 stars by the strength of their He II λ4686 emission (the source of the "f" in the spectral designation), the strength of N IV λ4058 emission (the source of the "*"), and the strength of the N V λλ4603, 4619 absorption feature. Like O3 stars of any luminosity class, the stars also show moderate He II λ4200 and λ4542 absorption with no indication of He I λ4471 or any other He I line. Walborn (1982) prefers the notation "O3 If*/WN6-A" to designate those O3 If* stars with the strongest emission lines as an indication that their spectra are in some ways intermediate between an O3 and a Wolf-Rayet WN type. Conti (1988) further describes these objects and argues that these are truly in transition from O-type to WR-type. We note that there really is a continuum, however, of the strengths of the emission lines. Among the eight R136 O3 If* stars, R136-044 and R136-015 show the strongest emission, and R136-036 and R136-016 show the weakest. We illustrate representative spectra in Figure 3. As the He II λ4686 and N IV λ4058 emission lines become stronger, the N IV λ3480 line follows suit, going from complete absorption into emission. Similarly, Hγ develops a P Cygni emission-line profile in both R136-015 (not shown) and R136-044. The spectra of these two stars resemble that of HD 93162, classified as a Wolf-Rayet star. Of our eight O3 supergiants, six have sufficiently strong emission to qualify as "transition" O3 If*/WN6-A type; see, for comparison, the spectrum of Sk −67°22, illustrated by Walborn (1986).

We see from Table 1 that these stars are all extremely luminous: values of M_V span the range −5.5 to −6.9. Interestingly, the two stars with the most extreme emission are not the most luminous, at least not as judged by their *visual* absolute magnitude. However, given the discussion above that O3 stars can span a range in $T_{\rm eff}$, and hence in bolometric correction, it may be that these two stars are the most *bolometrically* luminous.

3.2. *Lower Luminosity O3 Stars*

Lower luminosity O3 stars show weak or neutral He II λ4686 emission [luminosity class III(f*)] or He II λ4686 absorption (class V). Similarly N IV λ4058 is weak in emission in giants and missing in dwarfs. In the O3 III(f*) standard star HDE 269810, N V λλ4603, 4619 is present, albeit weakly. We do not see these N V absorption features in any but our luminosity class "If*" objects, which we believe is simply a S/N and resolution effect. Our O3 V stars are a good match to the O3 V "standard" HDE 303308 illus-

TABLE 1

SPECTRAL TYPES R136 CLUSTER

STAR[a]	ρ[b] (pc)	M_V	SPECTRAL TYPE	
			New	Previous[c]
2 = Mk42	1.9	−6.8	O3 If*/WN6-A	O3 If*/WN6-A (WB97)
4 = R134	2.8	−7.1	WN6 (with H)	WN7 (M85)
6 = R136a3	0.1	−7.1	WN4.5 (with H)	O3f/WN (deK97)
7 = Mk39	2.9	−6.9	O3 If*/WN6-A	O3 If*/WN6-A (WB97)
8 = Mk34	2.5	−7.0	WN4.5 (with H)	WN4.5 (M85)
9	0.5	−6.9	O4 If+	…
10	0.8	−6.8	WN4.5 (with H)	…
11 = Mk37W[d]	2.8	−6.6	O4 If+	WN7: (M85)
12 = Mk35	3.0	−6.3	O3 If*/WN6-A	O3 If*/WN6-A (WB97)
13 = Mk32[d]	4.5	−6.2	O8 III(f)	O7.5 II (WB97)
14 = Mk37	2.9	−6.5	O4 If+	O4 If(M85)
15 = Mk30	4.0	−6.1	O3 If*/WN6-A	O3 If*/WN6-A(WB97)
16 = Mk33[c]	3.2	−6.2	O3 If*	O4:(M85)
18 = Mk33S[c]	2.7	−6.0	O3 III(f*)	WC5+OB(M85)
20 = R136a5	0.1	−6.0	O3 If*/WN6-A	O3f/WN (deK97)
23 = Mk35S	3.5	−5.6	O3 III(f*)	O4–5 V: (WB97)
24 = R136a7	0.1	−5.8	O3 III(f*)	…
25	4.0	−5.5	O3 V	…
28	1.8	−5.5	O3 V	…
29	1.2	−5.2	O3 V	…
30	0.1	−5.4	O7 V	…
32	3.2	−5.4	O6.5 V	…
33	0.6	−5.3	O3 V	…
34	2.8	−5.1	WC5	…
35	0.2	−5.2	O3 V	…
36	0.4	−5.5	O3 If*	…
37	2.4	−5.5	O3 III(f*)	…
38	1.2	−5.3	O3 III(f*) + O8:	…
39	0.4	−5.2	O4 V((f)) + O6:	…
40	0.4	−5.2	O3 V	…
41 = Mk35N	2.2	−5.2	O3 III(f*)	O8:V (WB97)
42	0.4	−5.1	O3 V + O3–5 V	…
43	3.9	−5.1	O3 V	…
44	2.9	−5.6	O3 If*/WN6-A	…
45	0.6	−5.2	O3 V	…
47	0.4	−5.3	O3 III(f*)	…
48	0.3	−5.2	O3 III(f*)	…
49	0.4	−5.0	O3 V	…
51	2.5	−4.9	O3 V	…
52	0.3	−4.9	O3 V	…
53	4.9	−4.6	O6 V	…
55	0.5	−5.0	O3 V	…
57	0.9	−5.5	O3 III(f*)	…
58	0.1	−4.9	O3 III(f*)	…
59	1.0	−5.3	O3 III(f*)	…
64	0.5	−4.8	O7 V((f))	…
66	0.2	−4.7	O3 V	…
68	1.1	−4.9	O3 V	…
69	0.3	−4.3	O3–6 V	…
71	0.5	−4.3	O3–6 V	…
73	0.3	−4.5	O9 V	…
74	4.5	−4.5	O6 V	…
77	0.3	−4.5	O3 V + O3 V	…
83	2.0	−4.3	O6 V	…
90	0.2	−4.3	O5::V	…
92	0.2	−4.2	O3 V	…
94	0.3	−4.1	O3 V	…
99	1.5	−4.1	O8 V	…
100	2.9	−4.2	B0 V	…
102	1.1	−4.6	O3 V	…
109	5.0	−3.7	O8 V	…
112	0.2	−4.0	O8.5 III(f)	…
113	2.3	−3.9	O9 V	…
H96-28 = Mk14	5.7	−5.5	O3 III(f*)	O3–6 V: (WB97)
H96-59 = Mk14N	5.1	−4.9	O5 V((f))	O4 V (WB97)

[a] Identification numbers are from Hunter et al. 1997, with additional references to Melnick 1985 (Mk) and Weigelt & Baier 1985 (see also Heap et al. 1994 (R136a) and Hunter et al. 1996 (H96).

[b] ρ is projected distance from cluster center in pc.

[c] Previous spectral types are from Melnick 1985 (M85), de Koter, Heap, & Hubeny 1997 (deK97), and Walborn & Blades 1997 (WB97).

[d] Mk32 is the blend of stars 13 and 74; Mk33 is the blend of stars 16 and 32; Mk33S is the blend of stars 18 and 34; and Mk37W is the blend of stars 11 and 44.

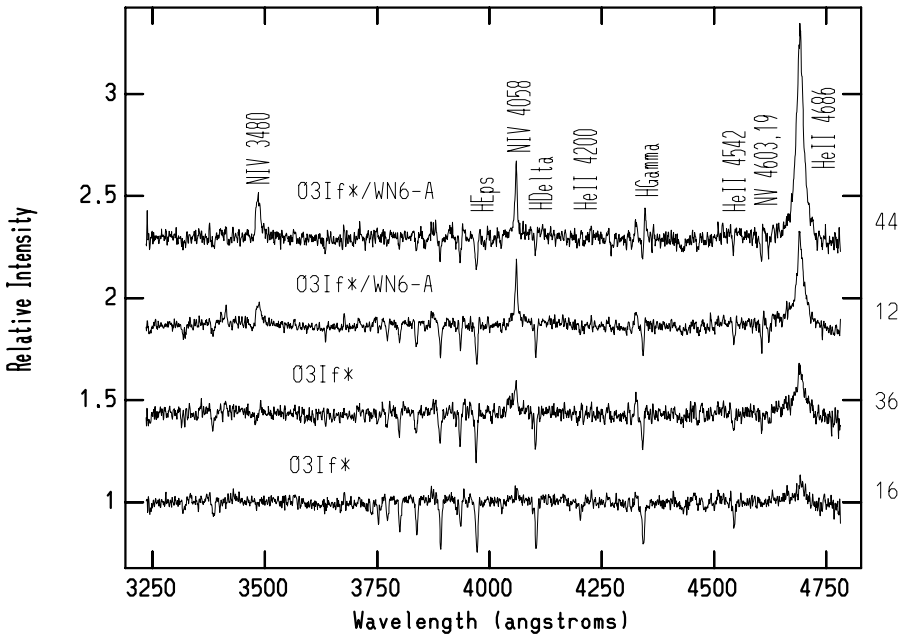

FIG. 3.—Representative examples of the O3 If* and O3 If*/WN6 supergiants. The emission feature on the blue side of Hγ is an artifact of the FOS, as is the extended blue wing to the N IV λ4058 line in star R136-036.

trated by Walborn & Fitzpatrick (1990) and Massey & Johnson (1993). Several examples of such stars are illustrated in Figure 4. Again we see that there is a smooth progression in the luminosity properties; compare with Figure 3. The visual absolute magnitudes in Table 1 range from $M_V = -4.9$ to -6.0 for the giants and $M_V = -4.1$ to -5.5 for the dwarfs; the overlap is understandable given the discussion above. Similarly, the most extreme O3 III(f*) star (based on the strength of the emission lines) is R136-057, which has intermediate M_V.

3.3. *The O4 Supergiants*

We have classified three stars as O4 supergiants, R136-009, R136-011, and R136-014. Their spectra are illustrated in Figure 5. R136-014 appears to be somewhat hotter than the other two, with less N III but more N IV emission. The presence of weak Si IV λλ4089, 4116 emission makes these all of spectral class O4 If+ (Walborn & Fitzpatrick 1990).

3.4. *High-Luminosity* H-*Rich WN Stars and a Bona Fide WC Wolf-Rayet Star*

The presence of Wolf-Rayet WN features, notably He II λ4686 and N III λλ4634, 4642 emission (also characteristic of "Of" stars) plus N IV λ4058 emission (also characteristic of O3 If* stars) was seen in ground-based spectra of the composite core of R136 (Ebbets & Conti 1982). The presence of WR stars in the region has also been taken as evidence of an age of 3–4 Myr for the R136 cluster (De Marchi et al. 1993; Hunter et al. 1995, 1996), a value hard to reconcile with the

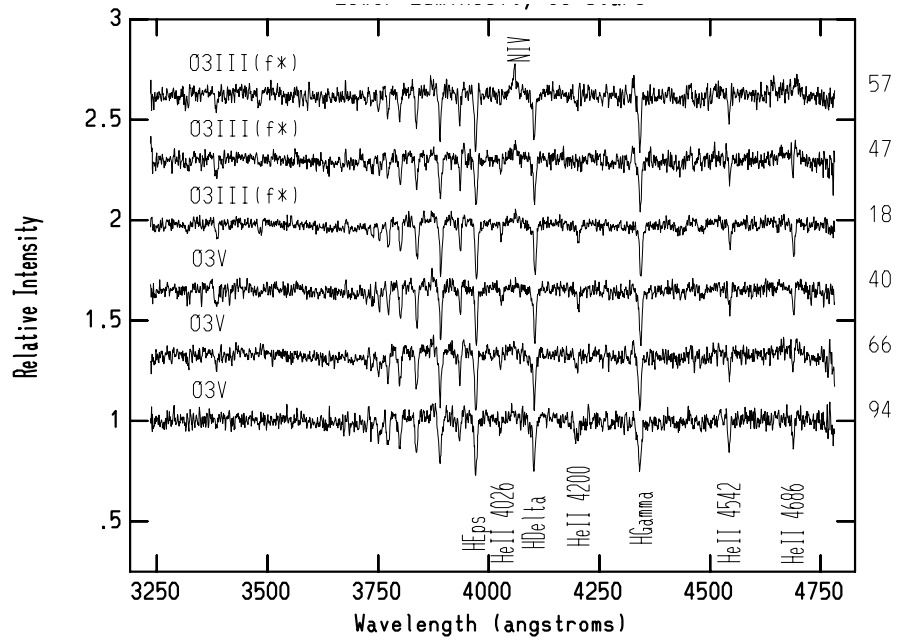

FIG. 4.—Representative examples of O3 giants and dwarfs. Note the weakness of the N IV λ4058 feature compared to that of the supergiants in Fig. 3.

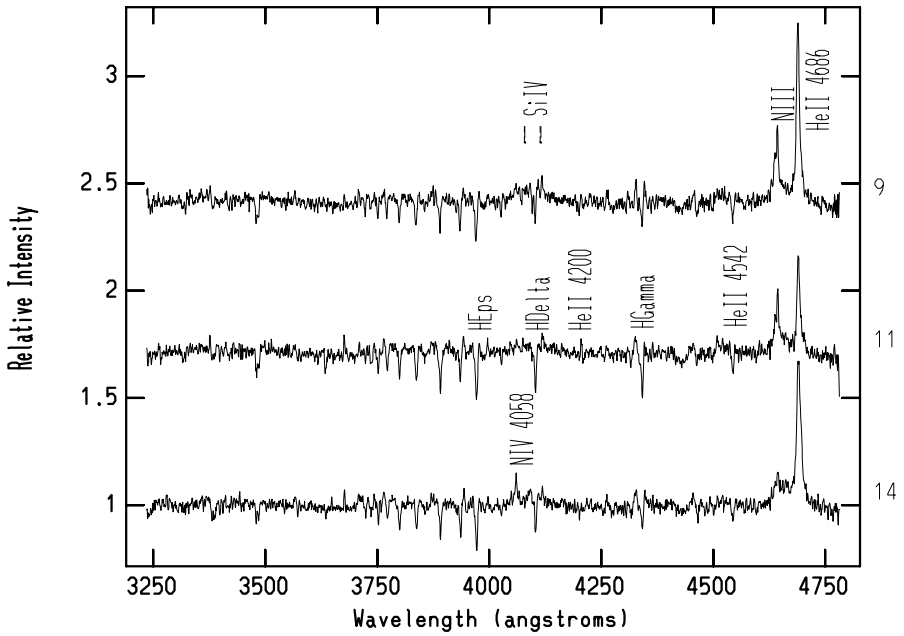

FIG. 5.—O4 If + stars show weak Si IV λλ4089, 4116 emission in addition to the extremely strong emission at He II λ4686 and N III λλ4634, 4642. The star R136-014 shows weaker N III but stronger N IV λ4058, making it intermediate between types O4 If and O3 If.

presence of stars in an O3 phase, which can't last more than 1 Myr or so.

Our spectroscopy revealed four WN stars, the spectra of which we show in Figure 6. Three of these (R136-006 = R136a3, R136-008 = Mk 34, and R136-010) have spectra that are nearly identical. The strength of N IV λ4058 and the weakness of N III λλ4634, 4642 leads to the WN4.5 classification. A fourth star, R136-004 = R134, is of slightly later type, WN6, as indicated by the similarity of strength of N III and N IV.

However, all four of these stars are unusual. First, all four show unmistakable evidence of hydrogen: the even-*N* Pickering He II transitions (coincident in wavelength with the Balmer hydrogen lines) are stronger than the neighboring odd-*N* Pickering lines (e.g., He II λλ4200, 4542). In fact, the three WN4.5 are incredibly H rich. Although, as a rule, some late-type WN stars (usually WN7 and WN8, but also some WN6 stars) show hydrogen, few of the known early-type WNs do (Conti, Leep, & Perry 1983). Secondly, violet absorption edges are visible for the WN4.5 stars at He II λ4542 and N V λλ4603, 4619; for the WN6 star, violet absorption edges are seen at He I λ4471. Again, this is highly unusual; violet absorption edges are usually seen for He I λ4471 in WN8 stars but not in early-type WNs (Conti et al. 1983). Thirdly, all four stars are unusually luminous in M_V; we see in Table 1 that these stars are among the most

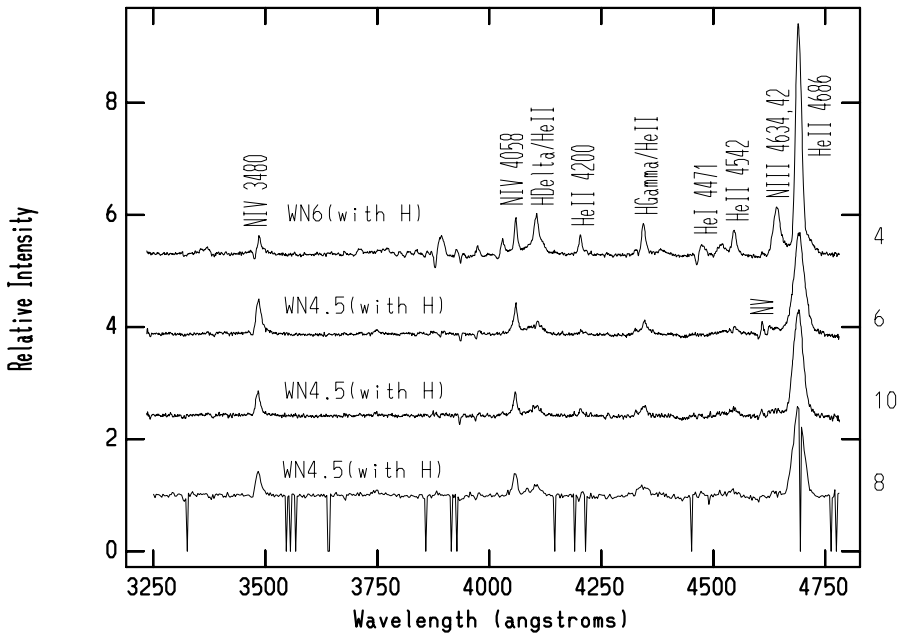

FIG. 6.—WN Wolf-Rayet stars. All four of these WN stars show evidence of H in their emission line spectrum, as judged by the alternating strengths of Hδ/He II, He II λ4200, Hγ/He II, and He II λ4542. The drop-outs in R136-008 are caused by dead diodes turned off in the FOS; this spectrum was not stepped but was obtained as part of the acquisition process.

luminous we've observed so far in R136. A typical WN4.5 should have an $M_v \approx -3.9$ on the narrow-band WR v photometric system (Table 7 of Vacca & Torres-Dodgen 1990, but converted to an 18.5 distance modulus); when allowance is made for the emission lines, this translates to a typical $M_V \approx -4.1$. *The three R136 WN4.5 stars observed here are more than a factor of 10 more luminous!* Even the WN6 star R134 is a magnitude more luminous than typical of its class.

The star R136-006 (R136a3) was recently the subject of a detailed analysis by de Koter et al. (1997), who used both FOS and GHRS spectra to conclude that the star is of very high mass, still in its core H-burning phase, but with a mass-loss rate that causes the spectrum to mimic that of a Wolf-Rayet. They classified the star as an O3 If*/WN type. While we do not believe that the spectral classification is defensible (there are, after all, no absorption lines present in the optical spectra, excluding the possibility of classifying it as an O3 If* star), we do however agree with the essence of their argument: we suspect that all three stars with WN4.5 spectra are extremely hot, highly luminous objects probably still in their core H-burning phases; their extremely high luminosities have resulted in WR-like mass-loss rates and hence in WR-like emission-line spectra. As such, they could be the logical extension of the "transition" O3 If*/WN stars discussed above. The situation with respect to the WN6 star is less clear, but this star could also be another "O3 star in Wolf-Rayet clothing."

This situation is reminiscent of the situation in NGC 3603, a "dense" cluster by OB association standards but which is sparse compared to R136. Drissen et al. (1995) used the FOS to obtain spectral classification of 14 luminous stars, of which three were classified as "WN6+abs." Examining their spectra obtained from the *HST* archives (see their Fig. 2), we would ourselves have been tempted to classify star "C" as a transition star, O3 If*/WN6-A, given an absorption spectrum of He II $\lambda\lambda$4200, 4542, Balmer lines, and N V $\lambda\lambda$4603, 4619. Their stars "A1" and "B" show strong H-rich spectra, and we note that their absolute magnitudes are comparable to that of the WNs discussed here, $M_V \approx -7.5$. The presence of WN stars, along with O3 stars, is as much a quandary in NGC 3603 as in R136, unless these WNs are actually H-burning objects. (See discussions in Conti 1996; Conti et al. 1995.)

We do find one bona fide WR star among our spectroscopic sample of R136, a WC star with fairly normal M_V (after correction for the very strong emission) and spectral features typical for an early-type (WC5) star. We note that this star is some 12″ (2.8 pc) from the cluster's core and could merely be seen in projection against the cluster rather than being physically associated with it.

3.5. *O Dwarfs*

Our spectroscopy shows a classical sequence of dwarfs, extending from the O3 V stars discussed above through B0 V. We show representatives of these in Figure 7. It is useful to compare these spectra to those of Melnick (1985) and of Walborn & Blades (1997), two ground-based studies conducted for the most part on stars further from the center of the nebula than these. In the ground-based studies, strong nebular emission at He I λ4471 made classification of these stars difficult, even with the advantages offered by linear detectors and long-slit subtraction. One further advantage enjoyed here of observations with a 0.″25 slit was the reduction of nebular contamination to the point that classification was straightforward. The sequence presented in Figure 7 is nearly a textbook example.

3.6. *Binaries*

Four double-lined binaries were apparent among our sample. The radial velocity shifts are large in all cases, with velocity separations of $\approx$600 km s^{-1}. This value is typical of massive binary systems with periods on the order of a few days (Garmany, Massey, & Conti 1980). Follow-up radial velocity and photometric monitoring has the potential of yielding masses directly for these very promising systems

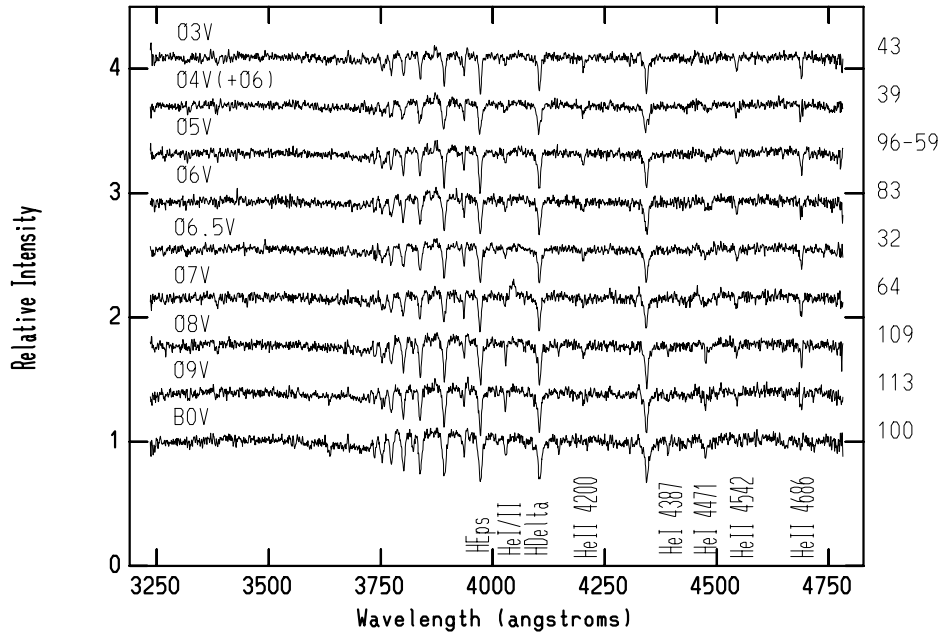

FIG. 7.—Representative spectra of the R136 dwarfs, extending from O3 V through B0 V. Note the noisy diode emission line in R136-064 near λ4050 and the effect of an intermediate low diode at λ4482, just redward of the He I λ4471 line.

(providing a much needed empirical check on the evolutionary models; see Burkholder, Massey, & Morrell 1997) and is being proposed.

R136-038 consists of an O3 III(f*) star (no He I λ4471) with a later type O star (strong He I λ4471, weak He II λ4542), probably of O8 type. The magnitude difference, measured from the Balmer lines (which are nearly constant in strength throughout the O spectral sequence) is 1.4 mag. At the time of the exposure, the radial velocity of the O3 III(f*) star was roughly -150 km s^{-1} with respect to the cluster, and that of the O8 star was $+400$ km s^{-1}.

R136-039 consists of an O4 V((f)) star plus a fainter ($\Delta m = 0.7$ mag) star of mid-O type, probably O6. At the time of the observation, the radial velocity of the O4 star was -200 km s^{-1} with respect to the cluster, and that of the O6 star was $+380$ km s^{-1}.

R136-042 consists of an O3 V star plus a slightly fainter ($\Delta m = 0.5$ mag) star also of early type—possibly as early as O3, but the radial velocity unfortunately places the He I λ4471 line in the region of the neighboring bad diode. The He II λ4542 lines are equally strong, suggesting that the companion has to be at least as early as O5. The radial velocities at the time of observations were -230 km s^{-1} and $+370$ km s^{-1}.

R136-077 appears to be two stars of nearly equal brightness, both of them of O3 V type. This is the only double-lined binary known containing two O3 stars (with the possible exception of R136-042, above). The radial velocities of the two components are also nearly equal, being -300 km s^{-1} and $+260$ km s^{-1} with respect to the cluster at the time of observation.

3.7. *Comparison with the Spectroscopy of Others*

We also give in Table 1 the spectral types determined from ground-based studies as well as from the de Koter et al. (1997) *HST* study. (Mk 42 was also observed in the ultraviolet by Walborn et al. 1992, who also called the star an O3 If*/WN6-A star, in agreement with the ground-based optical spectral type given by Walborn & Blades 1997.) The agreement is good when one remembers that the ground-based studies faced the problems of crowding (multiple stars masquerading as a single object at ground-based resolution) and nebular contamination, a particular problem for the He I λ4471 line, crucial for spectral classification of O-type stars. The obvious disagreements in spectral types are mainly understood in terms of blends, as given in the table notes.

Heap et al. (1994) and de Koter et al. (1997) observed two additional stars, R136a2 and R136a1, respectively, two components first resolved by ground-based speckle observations (Weigelt & Baier 1985). Neither of these was included in our program, as they are separated by only 0.″11 and are nearly equally bright at both F170W *and* F555W (stars 3 = R136a1 and 5 = R136a2 in Table 2 of Hunter et al. 1997). De Koter et al. (1997) decided to exclude the observation of R136a2 from their study because of contamination by R136a1 but retained R136a1; given the photometry of these stars, we expect that their analysis of R136a1 may have been affected by the spectrum of R136a2. However, unquestionably these stars are both extremely luminous and hot. The spectrum of R136a1 shown by de Koter et al. resembles that of our H-rich WN4.5 but with upper Balmer lines in absorption; that of R136a2 was called a weak-lined "WN4" on the basis of its UV spectrum.

4. CONVERSION TO EFFECTIVE TEMPERATURE AND LUMINOSITY

Although our discovery of so many O3 stars is exciting, we must transform this to quantitative information if we are to meet our goal of determining the initial mass function for the massive stars in the R136 cluster. In this section, we discuss the effective temperature scale for O stars and describe how we converted the spectroscopy and photometric information to physical parameters; i.e., log $T_{\rm eff}$ and $M_{\rm bol}$. Hunter et al. (1996) have already described this procedure for the intermediate-mass stars, using F336W, F555W, and F814W photometry; here we instead use the data set from Hunter et al. (1997), which includes observations in the F170W filter, as colors determined using this filter provide the strongest lever arm for determining the effective temperatures of the stars with only photometry.

4.1. *Stars with Spectra*

4.1.1. *The Effective Temperature Scale of O Stars*

Conti (1988) cautions that the effective temperature scale for O-type stars is uncertain at the 10% level. Vacca, Garmany, & Shull (1996) present an improved temperature calibration based upon recent results from the literature. This calibration differs from older temperature scales (Conti 1973, 1988; Chlebowski & Garmany 1991) primarily for the earliest type O stars. For instance, on the Chlebowski & Garmany (1991) scale, an O3 V star has $T_{\rm eff} \sim 48{,}500$ K and a bolometric correction of -4.4 mag and an O3 If star has $T_{\rm eff} \sim 44{,}500$ K and a bolometric correction of -4.1 mag. By contrast, Vacca et al. (1996) adopt values of $T_{\rm eff} \sim 51{,}000$ K and bolometric corrections of -4.6 mag for both O3 V and O3 If stars. Since massive stars evolve at fairly constant luminosity, the primary uncertainty in determining masses is caused by the uncertainties in the bolometric corrections. This effect can be illustrated from the following example. Using the evolutionary models of Schaerer et al. (1993) for an LMC-like metallicity, we would find that a star with $T_{\rm eff} = 51{,}000$ K and $M_{\rm bol} = -10.5$ mag (typical of an O3 If star using the calibration of Vacca et al. 1996) has a mass of 95 $\mathcal{M}_\odot$. If we had assumed values of $T_{\rm eff} = 44{,}500$ K and $M_{\rm bol} = -10.0$ mag (typical of an O3 If star using the Chlebowski & Garmany 1991 scale), we would have derived a mass of only 66 $\mathcal{M}_\odot$. The difference for O3 V stars, though, is relatively minor (80 $\mathcal{M}_\odot$ vs. 95 $\mathcal{M}_\odot$), and the differences become modest even for supergiants by spectral type O6.

One is tempted to naively attribute the difference between the Vacca et al. (1996) temperature scale and that of older studies to the improvements brought about by modern, sophisticated models that include many ions (for overviews, see Kudritzki & Hummer 1990; Kudritzki et al. 1992b); the "cooler" temperature scale is traceable to Conti (1973), who used the first non-LTE atmosphere models (Mihalas & Auer 1972), which included only H and He. However, this is to some extent an oversimplification. For instance, both Puls et al. (1996) and de Koter et al. (1997) have analyzed the UV and optical spectrum of Mk 42 (R136-002), one of the transition O3 If*/WN6-A stars discussed in § 3.1 above. Puls et al. find an effective temperature of 50,500 K, essentially the same as the 51,000 K value adopted by Vacca et al. for an O3 If star, while de Koter et al. derive 44,500 K for the same star, a number identical to the O3 If calibration of Chlebowski & Garmany (1991)! De Koter et al. and Heap

et al. (1994) find similarly "low" effective temperatures for R136a1, R136a2, and R136a5. Thus, although we provisionally adopt the Vacca et al. (1996) temperature scale, we will test our results by also using the cooler scale of Chlebowski & Garmany (1991).

No matter what calibration is assumed, we must also remember that the O3 spectral class is itself degenerate and that members of this spectral type must span a real range in effective temperature and hence in bolometric correction. For instance, detailed analysis by Kudritzki and collaborators have found values of $T_{\rm eff}$ ranging from 50,500 to 60,000 K (Kudritzki et al. 1992a, 1992b; for a recent summary, see Puls et al. 1996). The only *correct* way of understanding the physical parameters—even in a relative sense—of our O3 stars is to do the proper analysis with data that we are currently lacking; Hα is needed to derive the mass-loss rate, and UV data are needed to measure the terminal velocity, following the treatment outlined in Kudritzki et al. (1992b). Although we plan to obtain such data in the future, we adopt in the meantime a single value for the effective temperature and bolometric corrections for all of the O3 and H-rich WN stars.

4.1.2. *Reddening Corrections*

With an effective temperature scale established, we next appeal to the atmosphere models of Kurucz (1992) in order to determine the amount of reddening. As emphasized by Holtzman et al. (1995), the *HST* F336W, F555W, and F814W filters are sufficiently different from U, V, and I that it is necessary to perform any reddening correction in the WFPC2 system before converting to the standard system. In our case, we wish to determine "standard" $E(B-V)$ values as our ultimate goal is to determine bolometric luminosities by applying bolometric corrections, which are determined relative to standard values of M_V. The model calculations were carried out in Hunter et al. (1997); here we merely note that it was necessary to apply a -0.12 mag correction to the model F814W magnitudes in order to derive good agreement between the colors involving F814W and the others, as well as to provide consistency between the model and the observed reddening-free index $Q_{\rm uvi}$ as derived below. We list the adopted intrinsic colors as a function of spectral type in Table 2. By using the appropriate reddening models (Hunter et al. 1997) for R136, and applying these to the model fluxes, we then derive

$$\begin{aligned} E(B-V) &= E(F170W-F555W)/6.10 \\ &= E(F336W-F555W)/2.10 \\ &= E(F170W-F814W)/7.40 \\ &= E(F336W-F814W)/3.41\ . \end{aligned} \quad (1)$$

In practice, the four values of $E(B-V)$ derived this way were in excellent accord (average standard deviation 0.01 mag) and could be averaged.

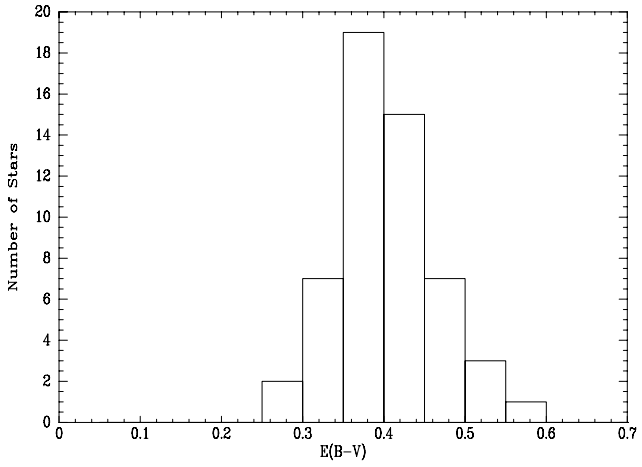

FIG. 8.—Histogram of the color excess $E(B-V)$ derived from the stars with spectroscopy.

For the Wolf-Rayet stars in Table 1, we did not deem it advisable to compute a reddening based upon the observed fluxes, given the possible effects of the emission lines. Instead, we found that the color excesses $E(B-V)$ determined from the other stars were spatially well correlated; i.e., neighboring stars had excellent agreement in $E(B-V)$ values despite the total range in $E(B-V)$ we observed. We therefore adopted the color excesses of the nearest neighbors for these stars. Similarly, we adopted the color excesses of the neighbors for any star in Table 1 with an uncertain spectral type. The average color excess for the remaining 54 stars is $E(B-V) = 0.40$, with the standard deviation of 0.06 providing a measure of the variation within the PC field. We show the histogram of the reddening in Figure 8.

4.1.3. *Conversion to $M_{\rm bol}$*

We next computed the absolute magnitude in the F555W system as

$$M_{F555W} = F555W - 18.5 - 3.2 \times E(B-V)\ ,$$

(where $R_{F555W} = 3.2$ is equivalent to $R_V = 3.1$) and then converted to an absolute visual magnitude in the Johnson V system by

$$M_V = M_{F555W} - 0.06\ ,$$

where the numerical constant was obtained using the transformation equations given by Holtzman et al. (1995) and is appropriate for hot stars. (Conversion to M_V is needed, as this is the basis for the bolometric corrections [BC].) Finally,

$$M_{\rm bol} = M_V + {\rm BC}\ .$$

TABLE 2

ADOPTED INTRINSIC COLORS

Spectral Type	$(F170-F555)_0$	$(F336-F555)_0$	$(F170-F814)_0$	$(F336-F814)_0$
O3–4	−4.24	−1.90	−5.73	−3.38
O5–7	−4.14	−1.87	−5.60	−3.33
O8–9.5	−3.93	−1.81	−5.38	−3.26
B0	−3.87	−1.75	−5.32	−3.20

4.2. *Stars without Spectroscopy*

For the stars without spectral types, we must make use of the photometry to determine the effective temperatures. As emphasized by Massey (1985), colors for hot stars are highly degenerate at UBV, and Massey et al. (1996) and Hunter et al. (1997) showed that this was true extending into the ultraviolet as well. Consideration of the Kurucz models and the photometric errors in Hunter et al. (1997) demonstrated that we had the greatest sensitivity to effective temperature if we corrected the photometry for reddening and then converted the intrinsic colors to effective temperatures, rather than relying on any of the possible reddening-free indices to transform to effective temperatures directly. However, this does require determining a value of $E(B-V)$ to better than 0.05 mag; otherwise, a determination of the effective temperature via an appropriate reddening-free index was more accurate. We used two methods to determine $E(B-V)$: (1) the average of the values of $E(B-V)$ for the nearest neighbors with spectroscopy, and (2) the use of a reddening-free photometric index, which is a good predictor of the intrinsic color. We found that the following relations worked well:

$$Q_{uvi} = (F336W-F555W)-1.60\times(F555W-F814W)$$

$$(F170W-F555W)_o = -5.458 + 2.923\times Q_{uvi}$$

$$(F170W-F814W)_o = -7.057 + 3.211\times Q_{uvi}$$

$$(F336W-F555W)_o = -2.558 + 1.466\times Q_{uvi}$$

$$(F336W-F814W)_o = -4.157 + 1.754\times Q_{uvi}\ .$$

We combined these with equation 1 to derive values for $E(B-V)$ and averaged the results. In most cases, the "neighbor method" and the "photometric method" produced very similar answers, which were combined and used to derive the intrinsic colors via equation 1. We then determined effective temperatures according to the following relations:

$$(F170W-F555W)_o = 121.984-52.6225\times\log T_{\rm eff} + 5.48146\times(\log T_{\rm eff})^2$$

$$(F170W-F814W)_o = 134.504-58.5148\times\log T_{\rm eff} + 6.10159\times(\log T_{\rm eff})^2$$

$$(F336W-F555W)_o = 77.089-33.5854\times\log T_{\rm eff} + 3.57025\times(\log T_{\rm eff})^2$$

$$(F336W-F814W)_o = 88.496-38.9708\times\log T_{\rm eff} + 4.13275\times(\log T_{\rm eff})^2\ .$$

(These were better functional fits than fitting the effective temperatures in terms of the colors; the equations were simply inverted to find $T_{\rm eff}$.) Stars for which the reddenings were poorly determined [as judged by any disagreement between the photometric and neighbor methods of determining $E(B-V)$] were noted, and their temperatures were determined using reddening-free indices, roughly

$$Q_{uvi} = 2.48275\times(\log T_{\rm eff})^2 - 2.3402\times\log T_{\rm eff} + 5.560\ .$$

We tested these relations by using the stars with spectroscopy and comparing the effective temperatures determined by assigning spectral classes to what we would have found by relying on photometry alone. There were no systematic errors, although there were differences in the effective temperatures that could amount to as much as 0.1 in $\log T_{\rm eff}$, or about 0.5 mag in the BC. We did find that the long baseline of $(F170W-F814W)$ made it an unreliable measure of the effective temperature simply because the demands on knowledge of the reddening became excessive. Instead, we simply averaged the other three to determine the effective temperature. The bolometric correction was then determined by

$$\mathrm{BC} = 27.66-6.84\times\log T_{\rm eff}.$$

5. THE H-R DIAGRAM, STAR FORMATION HISTORY, AND THE INITIAL MASS FUNCTION OF THE R136 CLUSTER

We are now prepared to answer the questions raised in the introduction, *how has star formation proceeded in the R136 cluster, and what is the initial mass function for massive stars in R136*. We begin by constructing the H-R diagram and use evolutionary models to determine ages and masses. We can then construct the initial mass function for the massive stars and compare the number of very massive stars to what we would have expected from the intermediate-mass stars studied by Hunter et al. (1996).

5.1. *The Most Luminous and Massive Stars*

We present our H-R diagram in Figure 9*a*. Stars with known spectral types are denoted by filled circles; stars with only photometry are denoted by open circles; and stars whose reddening is uncertain are indicated by plus signs. The curious "wall" of stars on the left of the diagram is an artifact of adopting a single temperature for the O3 stars; as discussed above, full analysis is needed on a star-by-star basis to remove the degeneracy of the O3 spectral classification.

We see immediately that the R136 cluster contains a large number of extremely massive stars. We list in Table 3 the most bolometrically luminous members. We have used the evolutionary tracks of Schaerer et al. (1993) to determine the (zero-age) masses of these stars. Since the evolutionary calculations extend only as high as 120 $\mathscr{M}_\odot$, beyond this we have had to extrapolate the mass using the mass-luminosity relation derived from the models.

What if we had used the cooler effective temperature scale of Chlebowski & Garmany (1991) instead? We show that H-R diagram in Figure 9*b* and include the masses and luminosities derived from these results in Table 3, as well. We see that irrespective of which temperature scale we adopt, the number of high mass stars in R136 is unprecedented.

It is interesting to see that the H-rich WN stars are the most bolometrically luminous stars in Table 3, at least when we adopt a constant bolometric correction for the O3 If*, O3 If*/WN6-A, and WN classes. This result is consistent with the argument that these are really "super O stars" whose extremely high luminosities have resulted in exceptionally strong stellar winds and a WN-like spectral appearance. The O3 If*/WN6-A and O4 If + stars are the next most luminous. We believe that the occasional exception to this trend in Table 3 is indicative of the inadequacies of adopting a single effective temperature and bolometric correction for the O3 supergiants and H-rich WNs.

5.2. *The Age of R136*

The ages inferred from these two H-R diagrams are considerably younger than the 3–4 Myr inferred by assuming

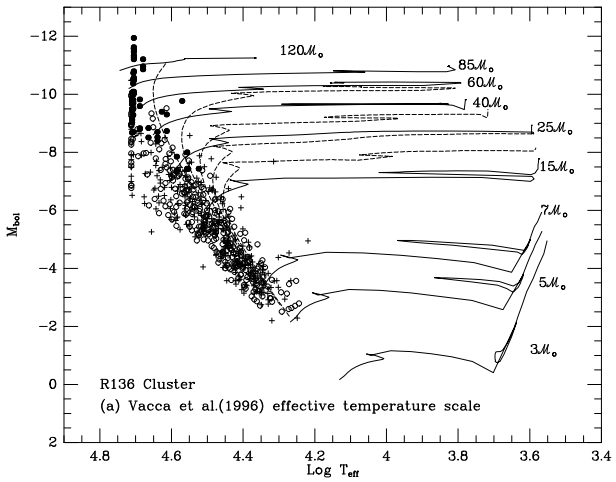

FIG. 9*a*

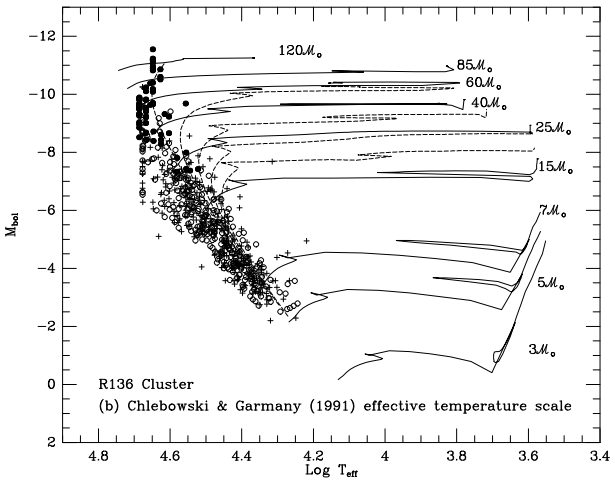

FIG. 9*b*

FIG. 9.—H-R diagram for the massive stars in R136. Filled circles are used for the stars with spectral types, and open circles are used for the stars with only photometry. The plus signs are used for stars whose reddening is uncertain. The evolutionary tracks of Schaerer et al. (1993) corresponding to the metallicity of the LMC are shown as solid lines, marked on the right by the zero-age main-sequence masses. The dashed lines are isochrones at 2 Myr intervals. In (*a*) we have adopted the "hot" temperature scale of Vacca et al. (1996), and in (*b*) we have used the "cool" temperature scale of Chlebowski & Garmany (1991). The scales differ only for the hottest stars.

that the WN stars are core He-burning objects. For the central core, we would infer a *very* young age, less than 1 Myr if the Vacca et al. (1996) temperature scale is adopted and less than 2 Myr if the cooler scale is adopted. This makes the R136 cluster not only the most populous cluster containing early-type stars ever studied but also possibly the youngest. There are several stars whose location in the H-R diagram suggest an age in excess of 2 Myr (specifically, the four points between the 40 $\mathcal{M}_\odot$ and 60 $\mathcal{M}_\odot$ tracks). Two of these are located well away from the cluster's center, with projected distances of 4.5 and 3.2 pc, which suggests the possibility that all four may simply belong to the more extended early-type population of the 30 Dor region and are seen in projection near the R136 cluster.

TABLE 3

THE MOST LUMINOUS AND MASSIVE STARS IN R136

	VACCA ET AL. 1996		CHLEBOWSKI & GARMANY 1991		
STAR	M_{bol}	$M_\odot$	M_{bol}	$M_\odot$	TYPE
3 = R136a1	−11.9	155	−11.6	136	WN4.5 (with H)
5 = R136a2	−11.6	140	−11.2	122	(WN4:—with H?)
4 = R134	−11.6	137	−11.2	120	WN6 (with H)
6 = R136a3	−11.6	137	−11.2	120	WN4.5 (with H)
8 = Mk34	−11.5	133	−11.1	116	WN4.5 (with H)
10	−11.3	127	−11.0	112	WN4.5 (with H)
2 = Mk42	−11.3	124	−10.9	108	O3 If*/WN6-A
7 = Mk39	−11.2	121	−10.8	103	O3 If*/WN6-A
9	−11.2	121	−10.9	104	O4If+
11 = Mk37W	−11.0	115	−10.6	88	O4If+
14 = MK37	−10.9	108	−10.5	84	O4If+
12 = Mk35	−10.8	108	−10.4	80	O3 If*/WN6-A
16 = Mk33	−10.7	105	−10.4	80	O3 If*
15 = Mk30	−10.6	97	−10.2	71	O3 If*/WN6-A
26	−10.5	95	−10.3	78	...
18 = Mk33S	−10.5	95	−10.2	76	O3 III(f*)
19	−10.5	95	−10.3	78	...
20 = R136a5	−10.5	93	−10.1	68	O3 If*/WN6-A
21	−10.4	90	−10.2	75	...
24 = R136a7	−10.4	88	−10.1	71	O3 III(f*)
23 = Mk35S	−10.1	79	−9.8	62	O3 III(f*)
25	−10.1	78	−9.9	68	O3 V
44	−10.1	78	−9.7	57	O3 If*/WN6-A
37	−10.1	78	−9.8	62	O3 III(f*)
36	−10.0	77	−9.7	56	O3 If*
28	−10.0	77	−9.9	67	O3 V
31	−10.0	76	−9.7	62	...
57	−10.0	75	−9.6	56	O3 III(f*)
46	−9.9	75	−9.7	61	...

With this new determination of the age of the massive stars in R136, the story of how star formation has proceeded in the R136 cluster is easier to tell. Previously, Hunter et al. (1996) had been forced to argue that intermediate-mass stars were still forming long after the high-mass stars had formed, contrary to the paradigm in which the massive stars form last, shutting down further star formation in the molecular cloud. However, the new picture that emerges is in fact consistent with this paradigm. We know that some of the intermediate-mass stars formed at least 4–5 Myr ago, as this is the time required to reach the main sequence for the lowest mass main-sequence stars detected by Hunter et al. (1996). However, they also found stars that appeared to fall along the pre–main-sequence tracks, suggesting a range of younger ages, possibly as young as 1–2 Myr. Now, with the age of the massive stars placed at ~ 1 Myr, it appears that the massive stars, along with some intermediate-mass stars, have been the last to form in R136. Furthermore, these stars have very quickly dispersed the gas cloud from the immediate vicinity of the cluster so that no further star formation would be possible there now. Thus, R136 does in fact fit the standard picture for the progression of star formation in a star cluster. Even so, however, the ages of the stars, as far as observed, do suggest a short timescale over which this progression has taken place, possibly <4 Myr altogether, for stars extending in mass from 2.8 $\mathcal{M}_\odot$ to >100 $M_\odot$.

Although R136 is the focal point of the 30 Doradus nebula, it is not the only recent star formation that has taken place there. Because 30 Dor covers a very large area on the sky, the stellar population of the region has only been sparsely sampled. However, blue stars, O-type stars, and *normal* Wolf-Rayet stars have been identified to at least a radius of 20′ from R136 (Hyland et al. 1992; Schild & Testor 1992; Parker & Garmany 1993). Detailed age analysis has not been done, but the presence of early O-type stars and their descendants argues that there were pockets of star formation that were roughly coeval with the formation of the super star cluster R136 itself. While the super star cluster was forming, the molecular cloud also formed numerous other associations of stars that are very much less rich and spatially compact.

Now, however, very little star formation appears to be taking place. Hyland et al. (1992) and Rubio, Roth, & Garcia (1982) have identified about 20 protostars within a few arcminutes of R136; these are likely to be the result of stellar winds compressing remnant cloud material. However, while a limited amount of such star-induced star formation is still taking place in the region around R136, for the most part star formation appears to be at a standstill. There is also evidence that some star formation took place in 30 Doradus of order 20 Myr ago. Hyland et al. (1992) found red supergiant stars spread throughout a region of about 5′ in radius, with the number of red stars dropping off dramatically outside that region. They interpret this as a population of older stars that formed in the 30 Doradus region previously. Some star formation has happened between this era and the formation of the R136 cluster: Walborn & Blades (1997) identify a cluster to the northwest with an age of 10 Myr and several regions with ages of 4–7 Myr. Thus, the broad-brush picture that we piece together from the currently available data is one in which there was some star formation about 20 Myr ago, followed by multiple sites of star formation taking place over the past 10 Myr, and essentially no substantive star formation taking place today. Thus, R136 and its environs may represent the culmination of star formation in the immediate 30 Doradus region.

5.3. *The Initial Mass Function of the Super Star Cluster R136*

Is the preponderance of very high mass stars indicative of a top-heavy IMF, or is it simply the result of a very young age and an incredibly rich and dense stellar aggregate? We are now in a position to answer this question.

In Figure 10, we show the initial mass function for R136; the quantity ξ is the number of stars per unit logarithmic (base ten) mass interval per unit area (kpc^2). For the Hunter et al. (1997) photometry, plotted in Figure 9, we assume completeness down to 15 $\mathcal{M}_\odot$. We also do not include the stars with inferred masses >120 $M_\odot$, as this bin is open ended, and besides, the masses are an extrapolation. We derive an IMF slope of $\Gamma = -1.3 \pm 0.1$ using the masses determined via the Vacca et al. (1996) temperature scale. As expected, the slightly lower masses for the highest mass stars lead to a slightly steeper slope $\Gamma = -1.4 \pm 0.1$ using the calibration of Chlebowski & Garmany (1991). We have assumed a statistical weighting; i.e., that the random variations in the number of stars per mass bin N is $N^{1/2}$.

These IMF slopes are indistinguishable from a Salpeter (1955) IMF slope of $\Gamma = -1.35$, typical of OB associations in the LMC and Milky Way (Massey et al. 1995a, 1995b). *Thus it would appear that the large number of extremely massive stars in R136 is just what is expected.*

Our spectral types extend down only to 50 $\mathcal{M}_\odot$ or so; below this, we are dependent upon just the photometry to locate our stars in the H-R diagram. We know that this procedure is highly uncertain for stars hotter than $T_{\rm eff} \sim$ 30,000 K, corresponding to a zero-age main-sequence mass of 20 $\mathcal{M}_\odot$. Thus, let us examine this question another way, by seeing if the number of massive stars is what we expect from the IMF derived from the intermediate-mass stars by Hunter et al. (1996). The Hunter et al. study derived the IMF in successive annuli about the cluster core, covering the mass range 2.8–15 $\mathcal{M}_\odot$. Let us use these IMFs to predict the number of massive stars (50–120 $\mathcal{M}_\odot$) and see how this

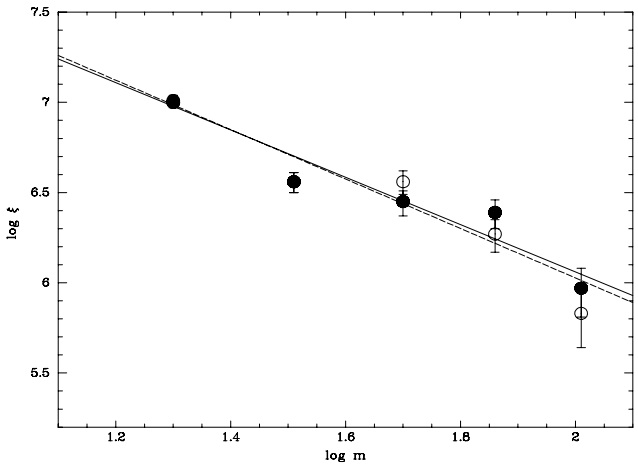

FIG. 10.—The initial mass function is shown for R136. The solid points and line use the Vacca et al. (1996) temperature scale, while the open points and dashed line are for the lower temperature Chlebowski & Garmany (1991) scale.

TABLE 4

NUMBER OF STARS WITH $\mathcal{M} = 50$–$120\ \mathcal{M}_\odot$

ANNULUS		IMF SLOPE	NUMBER	NUMBER OBSERVED	
(pixels)	(pc)	Γ	PREDICTED	Hot Scale	Cool Scale
10–30	0.11–0.34	-1.0 ± 0.4	9.7	11	10
30–40	0.34–0.46	-0.7 ± 0.4	7.2	8	8
40–60	0.46–0.69	-1.1 ± 0.3	5.9	4	5

compares with what is observed.[3] The results are given in Table 4. We again see excellent agreement.

The high masses in Table 3 are higher than the "upper mass cut-offs" found in normal Galactic and LMC OB association clusters (Massey et al. 1995a, 1995b). However, there are no other clusters studied that are this populous or this young. It may be that the very concept of an "upper mass cut-off" has to be considered carefully when talking about a coeval population; at what mass, consistent with age, does the IMF predict only one star?

Massey et al. (1995b) demonstrated that massive stars—even high-mass stars—are born *in the field* as part of modest star-forming events and that the IMF of these field stars is considerably steeper than Salpeter, with $\Gamma \sim -4$. The stellar density in the field is at least 2 orders of magnitude lower than that of the sparsest OB associations studied (Massey et al. 1995a). This suggests that star formation is not identical over *all* stellar density scales. But, it does appear to be remarkably similar over the 2 orders of magnitude in density estimated from a typical OB association to R136, a cluster comparable in stellar density to a globular cluster.

6. CONCLUSIONS AND SUMMARY

For a brief time in the early 1980s, it was believed by some that the semistellar core of the R136 cluster was itself a single supermassive (2000–3000 $\mathcal{M}_\odot$) star responsible for much of the ionization of the 30 Dor region (Cassinelli, Mathis, & Savage 1981). This interpretation was shaken by the resolution of R136a into multiple components from ground-based speckle observations (Weigelt & Baier 1985) and put to rest when the first *HST* images revealed these (and multiple other) components were of comparable brightness and color (Campbell et al. 1992). It is nevertheless interesting to note that Cassinelli et al. suggested that the alternative would require packing "on the order of 30 O3 or WN3 stars" within the R136 core. This was considered even less likely than the presence of a single object of several thousand solar masses (see discussion in Ebbets & Conti 1982). In retrospect, this paper was in fact prophetic: we note from Table 1 the confirmed presence of 39 O3 stars. This is considerably more than the total number of O3 stars identified in the Milky Way or elsewhere in the Magellanic Clouds.

Where Cassinelli et al. (1981) and others failed was in their assertion that the lower mass stars were missing in the R136 cluster, that somehow the IMF was peculiar. Our spectroscopy, combined with the photometry of Hunter et al. (1997), yields an IMF slope that is characteristic of far sparser OB associations seen in the Milky Way and Magellanic Clouds. The preponderance of extremely massive stars is no more, and no less, than what we would predict using the intermediate-mass IMF from the work of Hunter et al. (1996). It is simply the young age and richness of the cluster that results in such an unprecedentedly massive star population. Remarkably, the same IMF slope holds over the mass range from 2.8–5 $\mathcal{M}_\odot$ all the way to 120 $\mathcal{M}_\odot$ and over a stellar density range from that typical of OB associations to that typical of globular clusters.

In summary, then, our work has shown the following:

1. Spectroscopy of the 65 brightest, bluest stars reveals mostly the hottest O-type stars, those of type O3, including O3 If* supergiants and O3 If*/WN6-A transition stars. Even higher in luminosity than these are several H-rich WN stars. In agreement with the detailed analysis of de Koter et al. (1997), we conclude that these are core H-burning objects whose WR-like emission spectra are caused by their exceptionally high luminosities. We note that similar stars have been observed in the dense, young Galactic cluster NGC 3603 recently studied by Drissen et al. (1995).
2. The masses of the most luminous stars extend above 120 $\mathcal{M}_\odot$ (the highest mass for which evolutionary tracks are available), possibly as high as 140–150 $\mathcal{M}_\odot$. Detailed analysis is needed to firmly establish the physical parameters of the hottest stars, but it is certain that this cluster contains a large number of the most luminous and massive stars ever identified.
3. Nevertheless, the initial mass function from 15–120 $\mathcal{M}_\odot$ is completely normal ($\Gamma = -1.3$ to -1.4), and the number of stars in the mass range 50–120 $\mathcal{M}_\odot$ is in accord with the prediction from the intermediate-mass IMF.
4. The presence of so many O3 stars in the R136 cluster establishes that the massive star population is quite young (<1–2 Myr); this is consistent with the presence of WN Wolf-Rayet stars if indeed they are core H-burning objects. This young age for the massive stars now clarifies the story of star formation in the R136 cluster given by Hunter et al. (1996): the intermediate-mass stars began forming some 4 to 5 Myr ago and continued until the highest mass stars formed ~ 1 Myr ago, after which star formation appears to have ceased, in accord with the paradigm in which the massive stars form last.

The spectroscopy presented here would not have been possible without the accurate offsetting capabilities, fine spatial resolution, and excellent spectroscopic capabilities of the *HST*. We are grateful to the many astronomers and support personnel who made this possible, and in particular acknowledge David Soderblom, who originally suggested we use the blind-offsetting technique, and Jeffrey Hayes, who offered detailed planning advice. The various individ-

[3] There was an error in the IMF reported by Hunter et al. (1996) for the radial bin 0.11-0.34 pc in their Table 4. The correct values for log ξ in the four mass bins are 2.72, 2.65, 2.86, and 3.03, yielding a slope $\Gamma = -0.99$, rather than -0.79.

uals staffing the STScI's "help desk" (particularly Jen Christensen) were of use in understanding some of the peculiarities of the FOS. We also enjoyed conversations with Peter Conti on the interpretation of the spectra. Bill Vacca kindly extended the analysis of the Kurucz models used in Hunter et al. (1997) to include the F814W filter in order to accommodate the needs of the present study. Nolan Walborn provided useful comments. Support for this work was provided by NASA through grant number GO-06417.02-95A from STScI.

REFERENCES

Burkholder, V., Massey, P., & Morrell, N. 1997, ApJ, 490, 328
Campbell, B., et al. 1992, AJ, 104, 1721
Cassinelli, J. P., Mathis, J. S., & Savage, B. D. 1981, Science, 212, 1497
Chlebowski, T., & Garmany, C. D. 1991, ApJ, 368, 241
Conti, P. S. 1973, ApJ, 161, 181
———. 1988, in O Stars and Wolf-Rayet Stars, ed. P. S. Conti & A. B. Underhill, NASA SP-497 (Washington, DC: NASA), 81
———. 1996, in Wolf-Rayet Stars in the Framework of Stellar Evolution, ed. J. M. Vreux, A. Detal, D. Frainpont-Caro, E. Gosset, & G. Rauw (Liege: Inst. Astrophys.), 655
Conti, P. S., Hanson, M. M., Morris, P. W., Willis, A. J., & Fossey, S. J. 1995, ApJ, 445, L35
Conti, P. S., Leep, E. M., & Perry, D. N. 1983, ApJ, 268, 228
de Koter, A., Heap, S. R., & Hubeny, I. 1997, ApJ, 477, 792
De Marchi, G., Nota, A., Leitherer, C., Ragazzoni, R., & Barbieri, C. 1993, ApJ, 419, 658
Drissen, L., Moffat, A. F. J., Walborn, N. R., & Shara, M. M. 1995, AJ, 110, 2235
Ebbets, D. C., & Conti, P. S. 1982, ApJ, 263, 108
Garmany, C. D., Conti, P. S., & Massey, P. 1980, ApJ, 242, 1063
Heap, S. A., Ebbets, D., Malumuth, E. M., Maran, S. P., de Koter, A., & Hubeny, I. 1994, ApJ, 435, L39
Holtzman, J. A., Burrows, C. J., Casertano, S., Hester, J. J., Trauger, J. T., Watson, A. M., & Worthey, G. 1995, PASP, 107, 1065
Hunter, D. A., O'Connell, R. W., & Gallagher, J. S. 1994, AJ, 108, 84
Hunter, D. A., O'Neil, E. J., Lynds, R., Shaya, E. J., Groth, E. J., & Holtzman, J. A. 1996, ApJ, 459, L27
Hunter, D. A., Shaya, E. J., Holtzman, J. A., Light, R. M., O'Neil, E. J., & Lynds, R. 1995, ApJ, 448, 179
Hunter, D. A., Vacca, W. D., Massey, P., Lynds, R., & O'Neil, E. J. 1997, AJ, 113. 1691
Hyland, A. R., Straw, S., Jones, T. J., & Gatley, I. 1992, MNRAS, 257, 391
Kudritzki, R. P. 1980, A&A, 85, 174
Kudritzki, R. P., & Hummer, D. G. 1990, ARA&A, 28, 303
Kudritzki, R. P., Hummer, D. G., Pauldrach, A. W. A., Puls, J., Najarrow, F., & Imhoff, J. 1992a, A&A, 257, 655
Kudritzki, R. P., et al. 1992b, in Science with the Hubble Space Telescope, ed. P. Benvenuti & E. Schreier (Garching: ESO), 279
Kurucz, R. 1992, in The Stellar Populations of Galaxies, ed. B. Barbuy & A. Renzini (Dodrecht: Kluwer), 225
Massey, P. 1985, PASP, 97, 5
Massey, P., Bianchi, L., Hutchings, J. B., & Stecher, T. P. 1996, ApJ, 469, 629
Massey, P., & Johnson, J. 1993, AJ, 105, 980
Massey, P., Johnson, K. E., & DeGioia-Eastwood, K. 1995a, ApJ, 454, 151
Massey, P., Lang, C. C., DeGioia-Eastwood, K., & Garmany, C. D. 1995b, ApJ, 438, 188
Melnick, J. 1985, A&A, 153, 235
Mihalas, D., & Auer, L. H. 1972, ApJS, 24, 193
O'Connell, R. W., Gallagher, J. S., & Hunter, D. A. 1994, ApJ, 433, 65
O'Connell, R. W., Gallagher, J. S., Hunter, D. A., Colley, W. N. 1995, ApJ, 446, L1
Parker, J. Wm. 1993, AJ, 106, 560
Parker, J. Wm., & Garmany, C. D. 1993, AJ, 106, 1471
Puls, J., et al. 1996, A&A, 305, 171
Rubio, M., Roth, M., & Garcia, J. 1992, A&A, 261, L29
Salpeter, E. E. 1955, ApJ, 121, 161
Schaerer, D., Meynet, G., Maeder, A., & Schaller, G. 1993, A&AS, 98, 523
Schild, H., & Testor, G. 1992, A&AS, 92, 729
Simon, K. P., Jonas, G., Kudritzki, R. P., & Rahe, J. 1983, A&A, 125, 34
Vacca, W. D., Garmany, C. D., & Shull, J. M. 1996, ApJ, 460, 914
Vacca, W. D., & Torres-Dodgen, A. V. 1990, ApJS, 73, 685
Walborn, N. R. 1971, ApJ, 167, L31
———. 1982, ApJ, 254, L15
———. 1986, in Luminous Stars and Associations in Galaxies, ed. C. W. H. de Loore, A. J. Willis, & P. Laskarides (Dordrecht: Reidel), 185
———. 1994, in The MK Process at 50 Years, ed. C. Corbally, R. Gray, & R. Garrison (San Francisco: ASP), 84
Walborn, N. R., & Blades, J. C. 1997, ApJS, 112, 457
Walborn, N. R., Ebbets, D. C., Parker, J. W., Nichols-Bohlin, J., & White, R. L. 1992, ApJ, 393, L13
Walborn, N. R., & Fitzpatrick, E. L. 1990, PASP, 102, 379
Weigelt, G., & Baier, G. 1985, A&A, 150, L18